

Multiple Quantum Well Structures of Graphene

H. Sevinçli,¹ M. Topsakal,² and S. Ciraci^{1,2,*}

¹*Department of Physics, Bilkent University, Ankara 06800, Turkey*

²*UNAM-Institute of Materials Science and Nanotechnology, Bilkent University, Ankara 06800, Turkey*

Based on first-principles calculations we predict that periodically repeated junctions of graphene ribbons of different widths form multiple quantum well structures having confined states. These quantum structures are unique, since both constituents of heterostructures are of the same material. The width as well as the band gap, even the magnetic ground state for specific superlattices are modulated in direct space. Orientation of constituent ribbons, their width and length, the symmetry of the junction and their functionalization by adatoms are structural parameters to engineer electronic and magnetic properties of the quantum structure. Not only the size modulation, but also composition modulation such as the heterojunction of BN in honeycomb structure and graphene gives rise to confined states. Devices made from these graphene quantum structures display negative differential resistance.

PACS numbers: 73.22.-f, 72.80.Rj, 75.70.Ak

Recent advances in materials growth and control techniques have made the synthesis of the isolated, two-dimensional (2D) honeycomb crystal of graphene possible [1, 2, 3]. Owing to its unusual electronic energy band structure leading the charge carriers to resemble massless Dirac Fermions, graphene introduced novel concepts and initiated active research [1, 4, 5]. For example, quasi 1D graphene ribbons exhibit interesting size and geometry dependent electronic and magnetic properties [6]. Studies on the electronic structures of zigzag ribbons revealed partly flat bands near the Fermi level corresponding to two edge states with opposite spin polarization. These states attribute antiferromagnetic character and the ribbon becomes a half-metal under applied electric field [7].

Our study based on extensive first-principles [8] as well as empirical tight-binding (ETB) calculations [9] have shown that periodically repeating heterojunctions made of graphene ribbons of different width (and hence different band gaps) can form multiple quantum well structures. These superlattices are unique since both size and energy band gap, even the magnetic ground state for specific structures vary periodically in direct space. As a consequence, in addition to the propagating states, specific states are localized in certain regions. Localization increases and turns to a complete confinement when the extent of the ribbons with different widths increases. Widths, lengths, chirality of constituent ribbons and the symmetry of the junction provide variables to engineer quantum structures with novel electronic and transport properties. In particular, finite-size quantum structures can be combined to design various devices, such as resonant tunnelling double barrier (RTDB) or asymmetric Aharonov-Bohm loops. Once these devices are functionalized with transition metal atoms, the broken spin-degeneracy of states with energies $E_n(\mathbf{k}, \uparrow)$ and $E_n(\mathbf{k}, \downarrow)$, can be used for spintronics applications.

Bare and hydrogen terminated zigzag nanoribbons, ZGNR(n) (n being the number of carbon atoms in the

primitive unit cell) are semiconductors and the edge states give rise to antiferromagnetic ground state [7]. Their band gap, E_g decreases consistently as n increases for $n > 8$. However, armchair graphene nanoribbons, AGNR(n) display different behavior. The band gap [10] of bare ribbon varies with n ; it is small for $3(n/2) - 1$, but from $3n/2$ to $3(n/2) + 1$ it increases and passing through a maximum it becomes again small at the next minimum corresponding to $3(n/2) + 2$. As E_g oscillates with n its value decreases eventually to zero as $n \rightarrow \infty$. While AGNR(n) is paramagnetic, it can change to ferromagnetic ground state through decoration by transition metal atoms. Hydrogen terminated AGNR(18), which is normally a semiconductor, becomes a ferromagnetic metal upon decoration with Cr. It can be even half-metallic upon the adsorption of Co and Fe atoms. For example, once Cobalt adatoms are bonded to AGNR(18) with a binding energy of 0.8 eV the spin-degeneracy is broken; while majority spin bands are metallic with 100% spin polarization, the minority spin bands becomes semiconducting with a band gap of 0.5 eV.

The band gap values of bare AGNR(10) and AGNR(14) shown in Fig. 1 (a) and (b) are significantly different and are of 0.44 and 1.10 eV, respectively. Two different kinds of bands are distinguished by their charge density plots. These are bands of states having charge density uniformly distributed across the ribbon and those of edge states having their charge localized at both edges of the ribbon. Owing to the interaction between two edges of the narrow ribbon, the bands of edge states split. Upon termination of the carbon dangling bonds by hydrogen atom, the edge states disappear, and the energy band gaps are modified. While hydrogen terminated AGNR(10) has a narrow band gap of 0.39 eV, hydrogen terminated AGNR(14) has a wide band gap of 1.57 eV. In the rest of the paper all ribbons and superlattices are hydrogen terminated unless stated otherwise. As shown in Fig. 1(c), the value of rate of change of the

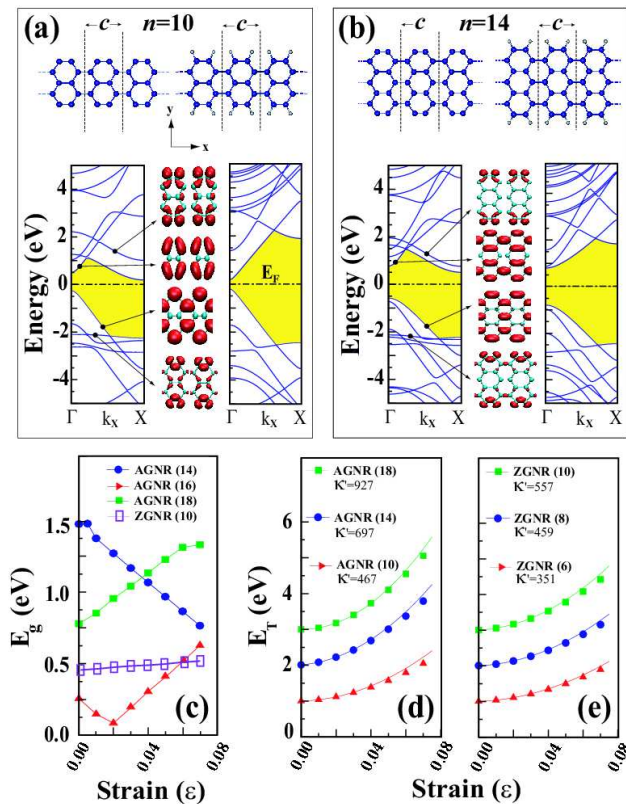


FIG. 1: (a) Bare and hydrogen terminated AGNR(10): Atomic geometry, electronic band structure and isosurface charge densities of edge and “uniform” states. The primitive unit cell is delineated with dashed lines and includes $n=10$ atoms. Carbon and hydrogen atoms are shown by large and small balls. Fermi level is set to the zero of energy. (b) Same for AGNR(14). (c) Variation of band gaps E_g of AGNR and ZGNR, with the tensile strain, ϵ . (d) Variation of the total energy of AGNR with ϵ and its second derivative with respect to ϵ , i.e. κ' . (e) Same as (d) for ZGNR. All data in this figure are calculated by first-principles method.[8]

band gaps with strain ϵ , i.e. $\partial E_g / \partial \epsilon$ is significant and its sign changes with n . It is interesting to note that while the band gap of ZGNR(10) increases by 13%, the edge magnetization increases by 18% when strain is applied by a value of % 7..

The mechanical properties of AGNR(n) and ZGNR(n) are investigated by calculating variation of total energy with strain, ϵ and its second derivative with respect to strain, $\kappa' = \partial^2 E_T / \partial \epsilon^2$. Results summarized in Fig. 1 (d) and (e) indicate that graphene nanoribbons are quasi 1D, stiff materials. For example, $\kappa' = 697$ eV/cell for AGNR(14). Interestingly, ZGNR(n) appear to be stiffer than AGNR(n) for the same n . These values can be compared with $\kappa = 127$ eV/cell calculated for linear carbon chain.

The variation of band gap with n and other properties of graphene ribbons discussed above are remarkable results which lead to heterojunctions with interest-

ing functions. Here the crucial issue to be addressed is whether the band gap discontinuity at the junction will result in confined (or localized) states. To this end we first consider a superlattice AGSL($n_1, n_2; s_1, s_2$) made by the segments of AGNR(n_1) and AGNR(n_2). Here, s_1 and s_2 specify the length of segments in terms of their numbers of unit cell. Fig. 2 shows a superlattice AGSL(10,14;3,3). It is made by periodically deleting one row of carbon atoms at both edges of AGNR(14) to form periodic AGNR(10)/AGNR(14) junction. Upon junction formation, dramatic changes occur in the band structure of this superlattice. Highest valence and lowest conduction bands are dispersive, but bands below and above the dispersive ones are simply flat. The isosurface charge density plots distinguish the different characters of these bands. For example, as highest valence band states propagate across the superlattice, the states of the second (flat) band are confined to the wider part of AGSL(10,14;3,3) consisting of AGNR(14) segment. These flat band states are identified as *confined* states.

Normally, a particular state, which is propagating in one region (or segment) is confined if it cannot find a matching state in the adjacent region having the same energy. For a superlattice of small n_1 or n_2 , spacings between energy levels are significant and hence localization of states in one of the regions is more frequent. This argument, which is relevant for superlattices of long constituent segments, may not be valid for short segments (or small s_1 and s_2). The confined states have been treated earlier in commensurate or pseudomorphic junctions of two different semiconductors, which form a periodically repeating superlattice structure [11]. These superlattices have grown layer by layer and form a sharp lattice matched interface. Owing to the band discontinuities at the interface, they behave as if a multiple quantum well structure obeying the Effective Mass Theory. Two dimensional conduction band electrons (valence band holes) confined to the well display a number of electronic and optical properties. In the present case, both the band gap and the size (width) of the graphene ribbon are periodically modulated in direct space and carriers are one dimensional. On the other hand the atomic arrangement and lattice constants at both sides of the junction are identical; the hetero character concerns only the width of the ribbons at different sides. Note that AGNR's can be constructed by using two different unit cells (i.e. those consisting of complete hexagons or of incomplete hexagons). For the wide region the one with complete hexagons is preferred in order to prevent a lonely carbon atom at the interface. For AGSL with reflection symmetry the narrow region is made by unicells having complete or incomplete hexagons depending on whether $(n_2 - n_1)/4$ is an even or odd number, respectively.

Electronic and transport properties of graphene multiple quantum well structures can be controlled by a number of structural parameters. In addition to $n_1, n_2, s_1,$

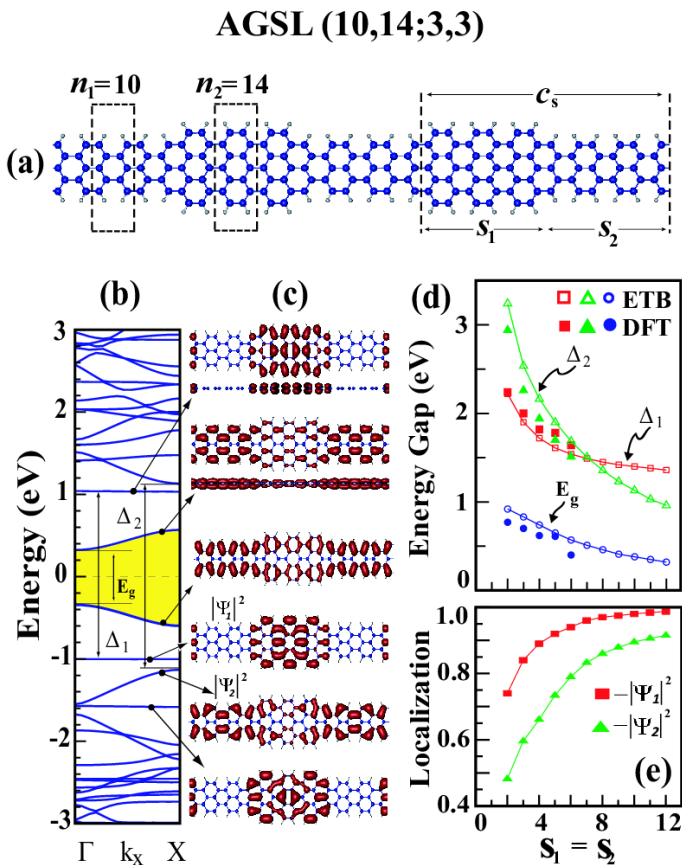


FIG. 2: (a) Atomic structure of the superlattice AGSL($n_1 = 10, n_2 = 14; s_1 = 3, s_2 = 3$). The superlattice unit cell and the primitive unit cell of each segment are delineated. (b) Band structure with flat bands corresponding to confined states. (c) Isosurface charge density of propagating and confined states. (d) Variation of various superlattice gaps with $s_1 = s_2$. (e) Localization of states versus $s_1 = s_2$.

s_2 , symmetry of the junction, $\Delta n = n_2 - n_1$, even-odd disparity of $n_1/2$ and $n_2/2$, type of the interface between two different ribbons and the shape of the superlattice (namely sharp rectangular or smooth wavy) influence the properties. As shown in Fig. 2 (d) as $s_1 = s_2$ increase, various superlattice band gaps decrease. Defining the localization as $\int_{s_2} |\Psi(\mathbf{r})|^2 d\mathbf{r}$, we see that confinement of states increase with increasing $s_1 = s_2$. For $s_1 = s_2 = 1$, confinement of specific states disappear. Differing of s_1 from s_2 causes E_g and the band structure to change. For example, the band gap of AGSL(10,14;4,2) is larger than that of AGSL(10,14;3,3). On the other hand, the energy of the flat bands of states confined in the s_2 region and their localization are practically independent of s_1 . Different values of n_1, n_2 result in a wide variety of electronic structures. For example, in contrast to AGSL(10,14;3,3) the highest valence and lowest conduction bands of AGSL(10,18;3,3) are flat bands with $E_g = 0.70$ eV; dispersive bands occur as second va-

lence and conduction band having a gap of 1.19 eV between them. The situation is even more complex for AGSL(10,22;3,3): While first and second bands are dispersive in both valence and conduction bands with a direct band gap 0.23 eV, flat bands occur as third bands with a gap of 2.61 eV between them. In all these cases the states associated with the flat bands near the Fermi level are confined at the wider part of the superlattice. Confinement in the narrow region of the superlattice is, however, less common. The above trends discussed for superlattices with small n_1 and n_2 become even more interesting when n_1, n_2 increase. We examined the electronic band structure and the confinement of states for wide superlattices, AGSL($n_1, n_2; s_1, s_2$) with $n_1 = 21$ or 41, but $n_2 > n_1$ and $s_1 = s_2 \geq 3$ using ETB method. For small Δn , confinement is weak and bands are dispersive, but confinement increases as Δn increases. Interestingly, E_g of AGSL($n_1 = 21, n_2; 3, 3$) is, respectively, 0.46, 0.12, 0.49 and 0.04 eV for $n_2 = 23, 25, 27$ and 29. Finally, electronic structure is also strongly dependent on the symmetry of the heterojunction. Here we distinguish symmetric (having reflection symmetry with respect to the superlattice axis along x -direction), asymmetric and saddle (one side is straight, other side is periodically caved) structures, which all have the same Δn . Our investigation on AGSL(10,18;3,3) reveals that while saddle structure has largest direct gaps between dispersive conduction and valence bands, symmetric structure has smallest gap, but largest number of confined states.

Superlattice structures formed from zigzag ribbons show also interesting properties. While zigzag ribbons ZGNR(8) and ZGNR(16) exhibit anti ferromagnetic ground states with opposite spin directions at both edges, their magnetic property undergoes a dramatic change upon superlattice formation. Apart from above features, which are characteristics of heterostructures, magnetic moments (having opposite directions) of the edge states of ZGSL(8,16;13/2,13/2) occur only in the narrow part of the superlattice, while their value become negligibly small at the wider part. Apparently, the magnetic moments are also modulated in the superlattice structure of zigzag ribbons. Such an interesting situation is a direct consequence of the confinement of magnetic edge states.

In addition to above heterostructure effects emerging from the modulation of the widths of constituent ribbons, compositional modulated superlattices within honeycomb structure can also be constructed. For example, BN honeycomb ribbons can match easily to graphene ribbons to form a multiple quantum well structure. We considered a periodic junction of the segment of armchair BN ribbon with $n_1 = 18$ and $s_1 = 3$ to the segment of armchair graphene with $n_2 = 18$ and $s_2 = 3$ to form a superlattice structure. While periodic BN and graphene ribbons by themselves have band gaps ~ 5 eV and 0.8 eV, the band gap of BN/AGNR(18) is 0.8 eV indicating a direct band alignment. In addition to compositional modulation, the

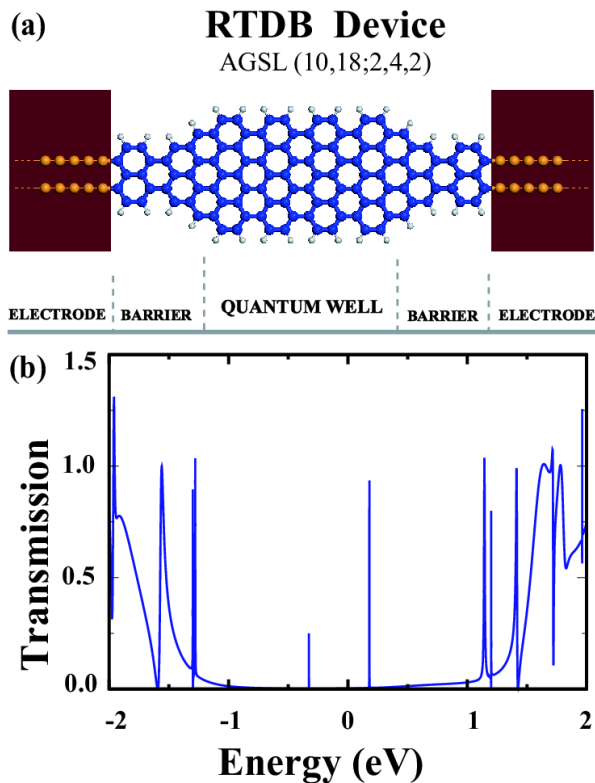


FIG. 3: (a) Atomic structure of a resonant tunnelling double barrier (RTDB) device made by the segments of AGNR(10) and AGNR(18) and connected to two metallic electrodes. (b) Transmission coefficient, T versus energy calculated under zero bias.

size modulation between the constituents gives rise to new changes in the electronic structure.

Finally, we show interesting transport properties of a quantum structure that can operate as a RTDB made by the junctions of AGNR(10) and AGNR(18) heterojunctions (See Fig. 3). For the sake illustration we considered fictitious metallic electrodes of two widely separated (weakly coupled) carbon chains[13] altogether having 4 quantum conductance channels and making perfect contacts with the central RTDB device. Six principal layers of electrodes are included at both sides of RTDB as parts of the central device. Transport properties are calculated self-consistently using non-equilibrium Green's Function method [14]. The transmission coefficient T , versus energy plot calculated under zero bias has sharp peaks, which originate from the resonant tunnelling through states confined to the quantum well. The confined states give rise to negative differential resistance in the I - V curve.

In conclusion, various types of quantum structures made by size and composition modulation of graphene based nanoribbons have been revealed. The confinement of spin-unpolarized or spin-polarized electron and hole states can lead to interesting effects, such as negative

differential resistance or spin-confinement. A richness of structural and compositional parameters to monitor electronic, magnetic and transport properties is expected to make these quantum structures an attractive field of research.

We acknowledge fruitful discussions with Dr E. Durgun. Part of the computations have been carried out by using UYBHM at Istanbul Technical University.

* Electronic address: ciraci@fen.bilkent.edu.tr

- [1] K. S. Novoselov, *et al.* Nature **438**, 197 (2005).
- [2] Y. Zhang, *et al.* Nature **438**, 201 (2005).
- [3] C. Berger, *et al.* Science **312**, 1191 (2006).
- [4] M.I. Katsnelson, *et al.* Nature Physics **2**, 620 (2006)
- [5] A.K. Geim and K.S. Novoselov, Nature Materials, **6**, 183 (2007).
- [6] Numerous studies have been carried out on the electronic structure of armchair and zigzag graphene ribbons. See for example: V. Barone, O. Hod and G.E. Scuseria, Nano Lett. **6**, 2748 (2006); Y.-W. Son, M.L. Cohen and S.G. Louie, Phys. Rev. Lett. **97**, 216803 (2006); M. Y. Han, *et al.* Phys. Rev. Lett. **98**, 206805 (2007).
- [7] Y-W Son, M.L. Cohen and S.G. Louie, Nature **444**, (2006)
- [8] We have performed first-principles plane wave calculations within DFT using PAW potentials [P.E. Blochl, Phys. Rev. B **50**, 17953 (1994)]. The exchange correlation potential has been approximated by Generalized Gradient Approximation (GGA) using PW91 functional [J. P. Perdew *et al.*, Phys. Rev. B **46**, 6671 (1992)] both for spin-polarized and spin-unpolarized cases. All structures have been treated within supercell geometry using the periodic boundary conditions. A plane-wave basis set with kinetic energy cutoff of 500 eV has been used. In the self-consistent potential and total energy calculations the Brillouin zone (BZ) is sampled by $(1 \times 1 \times 35)$ special \mathbf{k} -points for ribbons. This sampling is scaled according to the size of superlattices. All atomic positions and lattice constants are optimized by using the conjugate gradient method where total energy and atomic forces are minimized. The convergence for energy is chosen as 10^{-5} eV between two steps, and the maximum force allowed on each atom is 0.02 eV Å. Numerical plane wave calculations have been performed by using VASP package; G. Kresse and J. Hafner, Phys. Rev. B **47**, 558 (1993); G. Kresse and J. Furthmüller, *ibid* **54**, 11169 (1996).
- [9] C.H. Xu, *et al.* J. Phys.: Condens. Matter **4**, 6047 (1992).
- [10] As shown by the recent work based on self-energy corrections [L. Yang, *et al.* Phys. Rev. Lett. **99**, 186801 (2007)] the band gap, E_g is underestimated by the DFT calculations. Since we consider structures which have already a band gap, its actual value does not affect our discussion in any essential manner, but an enhancement of predicted properties (such as the extent of confinement) can be expected.
- [11] L. Esaki and L.L. Chang, Phys. Rev. Lett. **33**, 495 (1974).
- [12] Z.F. Wang, *et al.* Appl. Phys. Lett. **91**, 053109 (2007)
- [13] S. Tongay, *et al.* Phys. Rev. Lett. **93**, 136404 (2004)
- [14] Transport properties of RDTB device have been ana-

lyzed using Atomistix ToolKit version 2.2 within the method developed by M. Brandbyge, *et. al* Phys. Rev. **B65**, 165401 (2002). Double- ζ plus polarization numer-

ical orbitals have been used and atomic structures are further optimized before transport calculations.